Single Grating Reflective Digital Holography With Double Field of View

Byounghyo Lee, Changwon Jang, Dongyeon Kim, and Byoungho Lee, *Fellow, IEEE*

***Abstract*—Since 1960s, digital holography (DH) has been developed significantly as an exquisite optical sensing technique with its computational interpretation. Recent advances in the image sensor and the coherent light source have suggested the possibility of using DH in portable form that can be utilized in industrial fields. Field of view (FOV) should be sufficiently wide and the system be simple for successful landing of DH on the industrial market. To embody the possibility, in this paper, we present a method for implementing off-axis reflective DH using a single diffraction grating. Beam splitter and mirror in the conventional off-axis DH are replaced with a single diffraction grating. This replacement enables the implementation of simple interferometer while maintaining the performance of the holography. In addition, we apply the multiplexed illumination method to enhance space-bandwidth product of off-axis hologram. Using the wavelength dependence of the diffraction grating, the FOV can be doubled without additional optical element. We demonstrate the proposed method by three holographic imaging experiments with two laser diodes. The prototype provides lateral resolution of 19.69 μm with the FOV of 6.85 mm $\times$ 8.72 mm. The FOV is 1.9 times wider than the image sensor area of 6.85 mm $\times$ 4.59 mm. Overall size of the prototype is 12 cm $\times$ 17 cm $\times$ 5 cm, showing the suitability of implementation to the various industrial fields.**

***Index Terms*—Digital holography (DH), field of view (FOV), grating, off-axis DH, phase retrieval.**

I. Introduction

DIGITAL HOLOGRAPHY (DH) is a label-free imaging technique that can completely measure the complex amplitude of light using interference property [1]–[5]. The acquisition of complex amplitude provides various applications beyond the conventional imaging systems. For example, it allows to numerically propagate the wavefront over the measurement system's depth of field that enables quantitative investigation of three-dimensional (3-D) biological cells [6] and optical elements [7]. Despite the significant merits of DH, the performance and the complicated structure of interferometer were considered as main factors that hinder the system from a wide use in industry. With the recent development in technology such as small pixel size of the image sensor and high coherency of the light source, it is possible to implement the DH system using a few essential components [8]–[10]. Although these works alleviate the limitation by reducing the number of optical elements required, more simple and high-performance system is desired.

DH can be categorized in on-axis [11], [12] and off-axis [13], [14] configuration according to the angle of interference between signal and reference beams. The off-axis system collects data without any moving component. In addition, single-shot imaging can be adopted in the field of dynamic imaging and is known to be robust to experimental noises [15], [16]. To implement the off-axis DH system, an optical component that splits the beam and at least one additional optical component for tilting a beam are required. DH system that consists of a beam splitter and a mirror is a widely used method, but it would rather be more effective to replace these components with a single multifunctional element.

In the post processing of the off-axis DH, most of the frequency information is filtered in the Fourier domain to remove twin image and noises. Therefore, the filtered hologram contains relatively a small amount of space-bandwidth product (SBP) than that can be acquired by the image sensor. Although the off-axis configuration has useful advantages for practical applications, the limited SBP should be addressed. Frequency multiplexing that simultaneously records several different information in the remaining parts of frequency domain has been investigated to alleviate the SBP loss. This method is used in a variety of ways, such as reconstructing a phase profile with synthetic wavelength [17]–[20], acquiring a super-resolution image [21], [22], and capturing an image corresponding to multiple field of views (FOVs) [23]–[25]. Each multiplexed information should have a different carrier frequency to avoid signal aliasing. Therefore, the conventional multiplexing technique has a limitation that the system becomes complicated and bulky.

Here, we present a novel approach in constructing reflective off-axis DH system with a single diffraction grating as a multifunctional component. Since the grating can modulate incident beam of high quality, it has been widely used in DH field for extending the FOV [26]–[28], common-path configuration [29], [30], and diffraction phase microscopy [31], [32]. Although the previous studies have used the grating as an additional optical element, we adopt it to replace two essential components of conventional off-axis DH, a beam splitter, and a mirror. This

Manuscript received November 22, 2018; revised March 4, 2019; accepted March 13, 2019. Date of publication March 27, 2019; date of current version November 5, 2019. This work was supported by the Projects for Research and Development of Police Science and Technology under the Center for Research and Development of Police Science and Technology and Korean National Police Agency Grant PA-H000001. Paper no. TII-18-3094. *(Corresponding author: Byoungho Lee.)*

The authors are with the School of Electrical and Computer Engineering, Seoul National University, Seoul 08826, South Korea (e-mail: yui145263@snu.ac.kr; wkdckddnjs@gmail.com; dongyeon93@snu.ac.kr; byoungho@snu.ac.kr).

Color versions of one or more of the figures in this paper are available online at http://ieeexplore.ieee.org.

Digital Object Identifier 10.1109/TII.2019.2905646

substitution simplifies the interferometer by reducing the number of optical elements. The system becomes more robust to experimental noise because the degree of freedom in alignment is reduced. Moreover, the proposed method does not need a constraint on the specimen, such as sparsity, to use the signal beam as the reference beam because it takes the clear reference beam. We adopt wavelength multiplexing method to mitigate the limited SBP problem using two laser diodes (LDs). The single grating (SG) diffracts the incident beams at different angles as a function of wavelength. Although prior multiplexing research requires lots of optical elements for various propagation angles, proposed method can adopt the method even if two beams are in line. Thus, the proposed system does not need any additional optical components to make the beam of each wavelength propagate in a different angle.

In this paper, we apply the lensless DH technique for compact design [8], [33], [34]. Through the lensless method, wide FOV of hologram, which has a small optical aberration, can be obtained. To demonstrate the proposed method, three holographic imaging experiments are carried out using a 1951 USAF resolution target, a biological specimen, and a concave mirror. The size of prototype is 12 cm $\times$ 17 cm $\times$ 5 cm. The imaging performance shows resolution of 19.69 μm and FOV of 6.85 mm $\times$ 8.82 mm, 1.9 wider than the recording area of 6.85 mm $\times$ 4.59 mm. The proposed system shows the potential use in the biomedical and forensic fields with its high performance of quantitative phase retrieval.

II. Method

A. SG Off-Axis DH

When normally incident beam is reflected on the grating, it is split into several waves. The corresponding diffraction angles are

$$\theta_m = \sin^{-1}\left(m\frac{\lambda}{\Lambda}\right) \tag{1}$$

where $m = 0, \pm1, \pm2, \ldots,$ is the index of order, λ is wavelength, and Λ is grating period. An SGDH method in off-axis configuration is devised with zeroth and first orders of the diffracted beams. Fig. 1 shows the schematic diagram of the proposed system. The optical system consists of a coherent light source (LD), a lens, 1-D diffraction grating, and an image sensor. A diverging beam from LD is collimated by the lens and perpendicularly illuminated on the grating, as shown in Fig. 1(a). The incident beam on the grating is divided into ±1 orders, each of which diffracts in opposite angles. The blazed grating designed to have high grating efficiency in the -1st order is utilized to enhance interference efficiency. In this case, the $+1$st order of the beam directly enters the image sensor and is used as a reference beam. On the other hand, the -1st order of the beam is incident on the specimen and then reflected back to the grating with signal information. We set the specimen plane to have an angle with the reflected signal beam, as shown in Fig. 1(b). The normal vector of specimen is $\boldsymbol{n}$ and the angle difference between the specimen plane and the signal beam is $\boldsymbol{\delta} = (\delta_x, \delta_y)$. The reflected signal beam (s) has difference of $2\boldsymbol{\delta}$ with incident beam of the specimen, which results in off-axis configuration. Then,

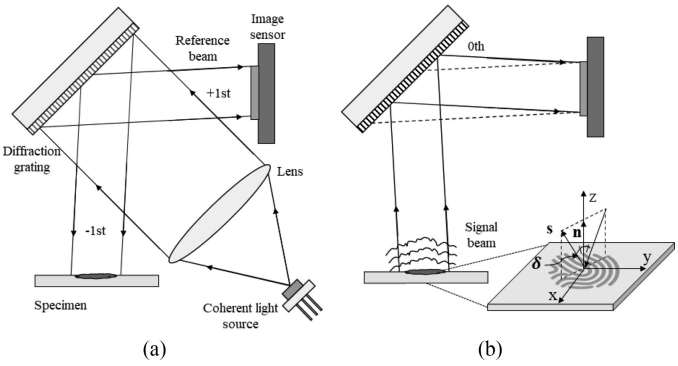

Fig. 1. SG off-axis reflective DH system. Only the beams detected on the image sensor are illustrated. (a) After collimated by a lens, normally incident beam is diffracted by the diffraction grating and split into reference and signal beams. (b) -1st order of beam is reflected on the specimen and interferes with the reference beam on the image sensor.

the signal beam is reflected by the grating through 0th order and propagated to the image sensor. In the image sensor, the signal beam and the reference beam make an off-axis interference pattern with a carrier frequency as

$$\nu = \frac{1}{\lambda}\sin(2\boldsymbol{\delta}) = \left(\frac{\sin(2\delta_x)}{\lambda}, \frac{\sin(2\delta_y)}{\lambda}\right). \tag{2}$$

The number of interference fringe pixel created by the carrier frequency should be more than 2 pixels to satisfy Nyquist sampling condition. Meanwhile, the number of pixels is also upper limited to mitigate signal aliasing and 3 to 4 pixels are reasonable compromise in practical implementation [35]. The angle difference $\boldsymbol{\delta}$ should be bounded by

$$\begin{aligned} \frac{1}{2}\sin^{-1}(\lambda/4p) &< \|\boldsymbol{\delta}\| \\ \max(|\delta_x|, |\delta_y|) &< \frac{1}{2}\sin^{-1}(\lambda/2p) \end{aligned} \tag{3}$$

where p is the pixel size of image sensor. The optical path difference (OPD) should be smaller than coherence length of light for interference. The reference beam reaches the image sensor directly after diffracted by the grating, but the signal beam experiences a longer optical path because of the additional round trip to the specimen. The OPD is about twice the distance between the grating and the specimen. In lensless DH, the specimen information of a wider area than that of the image sensor is measured due to diffraction of signal beam. Since most of the energy of the signal beam is concentrated on the dc component, we define the FOV as a bright field and the outer part is filtered during the reconstruction process. Therefore, the FOV is determined to be identical to the image sensor size.

B. Double FOV Implementation With Multiplexed Illumination

In Section II-A, we present a method to implement an efficient interferometer using a diffraction grating. Although SGDH provides an alternative interferometer with the fewer optical components, it is necessary to address the limited SBP of off-axis DH. In this section, a method to obtain a hologram of double SBP (double FOV with identical resolution) with a single-shot

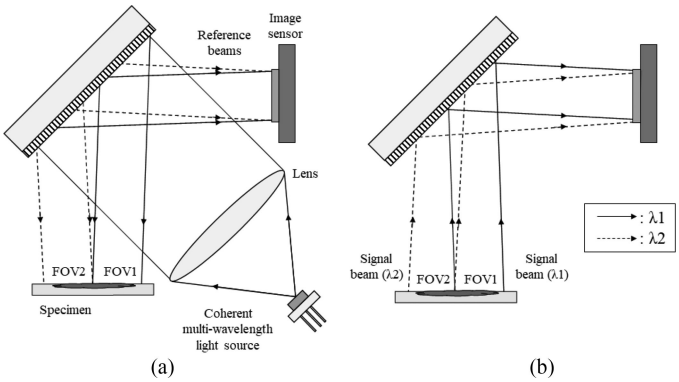

Fig. 2. SG with multiplexed illumination system. Note that only signal beams incoming to image sensor are illustrated. (a) Because diffraction angle depends on the wavelength, although two beams are incident on the grating with the same angle, they diffract in different directions. (b) Two signal beams of adjacent regions of FOV1 and FOV2 are reflected on the diffraction grating. The image sensor measures multiplexed hologram without additional optical components to change the carrier frequency.

configuration is introduced. The key idea is to use the remaining regions in the Fourier spectrum that are supposed to be filtered in conventional off-axis DH. Inspired by multiwavelength DH [17]–[20], we devise multiplexed illumination SGDH aiming for obtaining the hologram with double FOVs. Although methods for multiplexing FOVs have been proposed [23]–[26], they are not suitable for compact applications because the optical system becomes complicated and bulky to multiplex FOVs at different carrier frequencies. In our approach, however, diffraction grating makes it possible to apply the multiplexing method with its compact system. Fig. 2 shows the schematic diagram of the proposed double FOVs system. Combining multiwavelength light source with the lens, two plane waves that have different wavelength of λ_1 and λ_2 are illuminated on the grating, as shown in Fig. 2(a). The grating diffracts these waves in the angle of $\theta_{\pm 1,\lambda_1}$ and $\theta_{\pm 1,\lambda_2}$ according to (1), depending on wavelength. Since the diffraction angle from the grating is a function of wavelength, even if the light source system is constructed in line, the beams with two different wavelengths can reach different regions at different angles without additional optics for tilting and shifting. The two -1st order beams are sequentially reflected on the specimen and grating, as shown in Fig. 2(b). The reference and signal beams of two wavelengths (total four beams) make an interference pattern on the image sensor. When λ_1 and λ_2 are mutually incoherent, the measured intensity on the image sensor is given by

$$\begin{aligned} I(x,y) &= |R_{\lambda_1}(x,y)|^2 + |R_{\lambda_2}(x,y)|^2 + |S_{\lambda_1}(x,y)|^2 \\ &+ |S_{\lambda_2}(x,y)|^2 + R_{\lambda_1}(x,y)S_{\lambda_1}(x,y)^* + R_{\lambda_1}(x,y)^*S_{\lambda_1}(x,y) \\ &+ R_{\lambda_2}(x,y)S_{\lambda_2}(x,y)^* + R_{\lambda_2}(x,y)^*S_{\lambda_2}(x,y) \end{aligned} \tag{4}$$

where R_λ and S_λ are complex amplitudes of reference and signal beams of λ, and $*$ denotes conjugation operator. The sixth and eighth terms on the right-hand side of (4) can be decomposed separately by spatial frequency filtering. By designing the multiplexing system to satisfy the carrier frequency condition, we obtain holograms of two adjacent FOVs while keeping

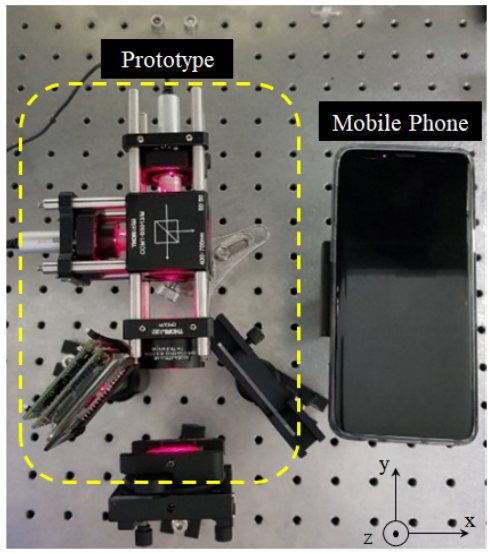

Fig. 3. Experimental setup of proposed method with multiplexed illumination. We combine two LDs for double wavelength illumination. The size of the system is measured in the area indicated by the yellow dashed line. The mobile phone is placed next to the system for size comparison.

a single-shot acquisition. In order that both FOVs correspond to adjacent regions without overlapping or discontinuance, the distance from specimen to the sensor should be satisfied

$$d = \frac{\mathrm{FOV}_y}{|\tan(\delta_{\lambda_1,y}) - \tan(\delta_{\lambda_2,y})|} \tag{5}$$

where FOVy is y-directional length of sensor, and $\delta_{\lambda,y}$ is y component of the difference angle with wavelength of λ.

III. Result

To demonstrate SGDH with multiplexed illumination, we carry out three holographic imaging experiments. A 1951 USAF resolution target, a latent finger print on slide glass, and a concave mirror are used as specimens. Fig. 3 is the experimental setup of the proposed system. The system consists of two LD modules (Thorlabs, CPS650F and CPS670F, wavelength of 650 and 670 nm), a plano-convex lens (Thorlabs, AC254-075-A-ML, focal length of 75 mm), a SG (Edmund, 43–210), and a CMOS sensor (Artray, 100MI-USB3-T2, pixel pitch of 3.34 μm). We merge the beams from LDs of two different wavelengths by implementing a beam splitter and a collimating lens to create two plane waves. Note that it is possible to substitute the merged light source with a single LD (without beam combining process) by using the commercialized dual or multiwavelength LD. The period of grating is 1200 grooves/mm, which diffracts two normal incidence beams in 51.3° and 53.5°, respectively. The diffraction efficiency varies with the angle between the polarization of incident beam and the direction of the grating vector. We measure the efficiency for all the linear polarization states and choose around 60° with grating vector where the reference beam and the signal beam are of similar intensity. With multiplexed illumination, a single multiplexed hologram is captured on 1376 $\times$ 1920 pixels of the sensor, which corresponds to 4.59 mm (H) $\times$ 6.41 mm (V). We set the angle difference

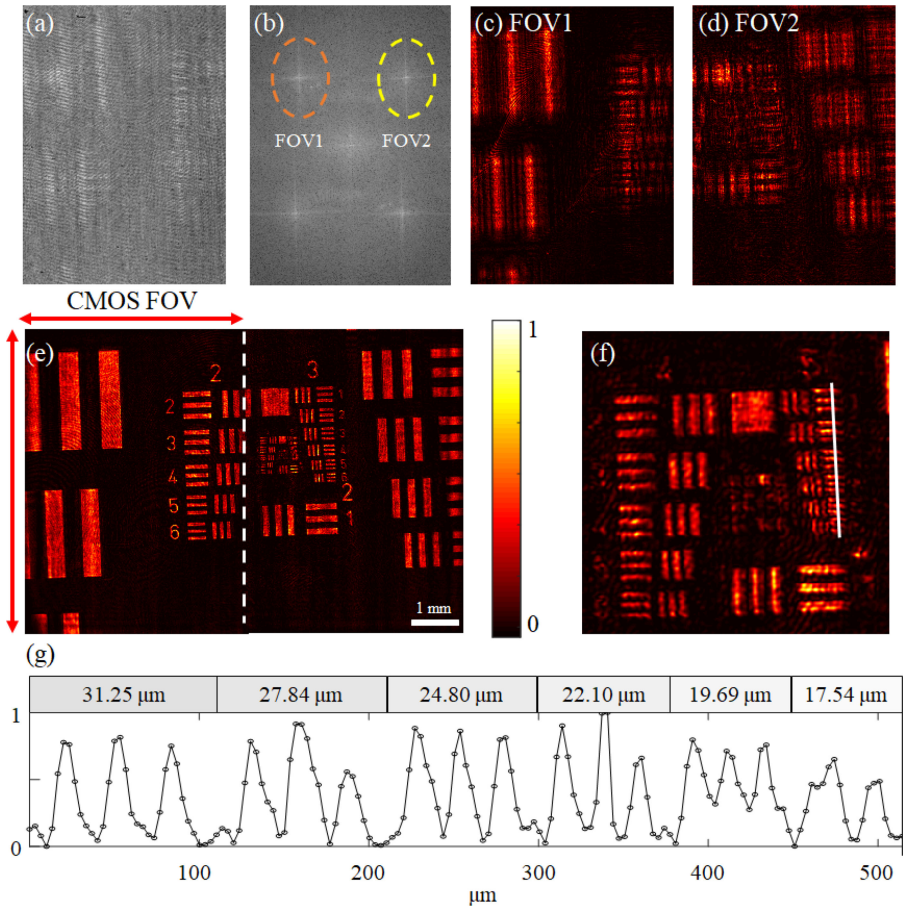

Fig. 4. Experimental results of 1951 USAF resolution target imaging. (a) Captured image using SGDH with multiplexed illumination. (b) Fourier spectrum of the captured image. The signals of different FOVs appear with different carrier frequencies. (c) and (d) Intensity images of the filtered regions in the spatial domain. Each filtered image is digitally propagated with its wavelength and makes the wide FOV of the hologram. (e) Stitched double FOV of the hologram. The size of image sensor is presented using the red arrows. (f) Zoom-in image that presents high-resolution part. (g) Cross section of the intensity through the vertical line of group 5, which corresponds to the white line in (f).

as $\boldsymbol{\delta}_{\lambda_1} = (1.5^\circ, -1.1^\circ)$ and $\boldsymbol{\delta}_{\lambda_2} = (1.5^\circ, 1.1^\circ)$. It makes signal spectrum of two wavelengths appear at the opposite sides from x-axis. In our prototype, amplitudes of the $\boldsymbol{\delta}$ are 1.86° for both wavelengths. From (3), the lower bounds are given by 1.39° and 1.44°, and the upper bounds are given by 2.79° and 2.88° for 650 and 670 nm, respectively. Therefore, our system satisfies both conditions. OPD of the prototype is about 10 cm, short enough to achieve interference pattern using LDs. Following (5), we set the distance from sensor to specimen as 10.5 cm to obtain the adjacent FOVs of holograms with a minute overlapping. Although the ideal distance is 11.7 cm, the overlapped region helps to stitch holograms and remove edge artifacts. When the distance from sensor to specimen (l) is smaller than d, the lateral overlapped ratio is given by $(100 - 8.4 \times l)\%$. The overall size of the prototype is 12 cm × 17 cm × 5 cm, corresponding to the area indicated by the yellow dashed line shown in Fig. 3. A mobile phone (Samsung, Galaxy 9) is shown to compare the form factor. We believe this comparison shows the potential that the proposed system can be applied to industrial fields in the form of a hand-carriable form.

Fig. 4 shows experimental results using a 1951 USAF resolution target (Edumund, 51–152). Fig. 4(a) and (b) shows the captured image and the Fourier spectrum of this image. As we set $\delta_{\lambda_1,y} = -\delta_{\lambda_2,y}$, two shifted signals appear at nearly opposite sides in x-axis and are sufficiently separated from each other. The signals are filtered around each carrier frequency considering the bandwidths. Fig. 4(c) and (d) are the frequency filtered images acquired by applying inverse Fourier transform to the noted regions of Fig. 4(b). In the reconstruction process, these holograms are digitally propagated to 10.5 cm through angular spectrum method with corresponding wavelength. Then, hologram with double FOV is acquired by stitching the two holograms, as shown in Fig. 4(e). The area of the image sensor is indicated by the arrows. In this experiment, we allow 10% overlapped region in lateral direction between two images to connect the images smoothly. The FOV of a synthesized image is 6.85 mm × 8.72 mm, which is 1.9 times larger than the image area of the sensor (6.85 mm × 4.59 mm). Fig. 4(f) is a magnified image of high-resolution parts of Fig. 4(e). To check the resolution of our system, we plot the cross section following the white vertical line. Element 5 of group 5 is resolved, which corresponds to resolution of 19.69 μm, as shown in Fig. 4(g). Abbe diffraction limit for coherent illumination is λ/NA, where NA denotes numerical aperture. As we measure high-resolution

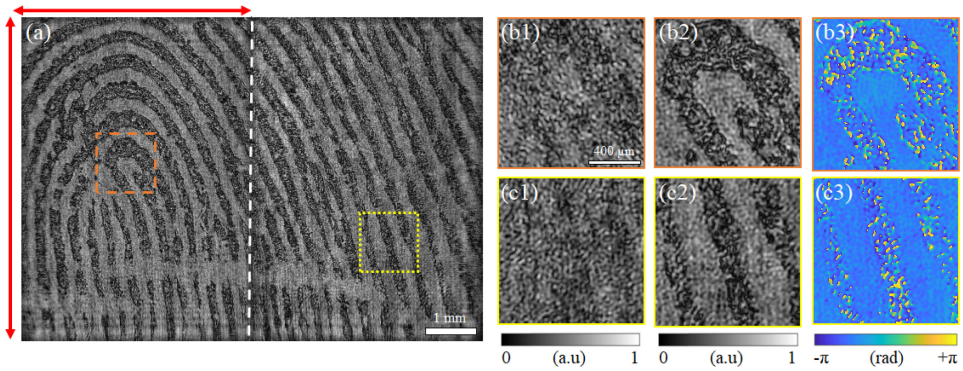

Fig. 5. Holographic imaging experimental results using the latent fingerprint. (a) Synthesized double FOV focused image. (b1) and (c1) Zoom-in intensity images corresponding to the noted boxes in (a) before the numerical propagation. Focused zoom-in (b2) and (c2) amplitude and (b3) and (c3) phase images reconstructed by numerical propagation.

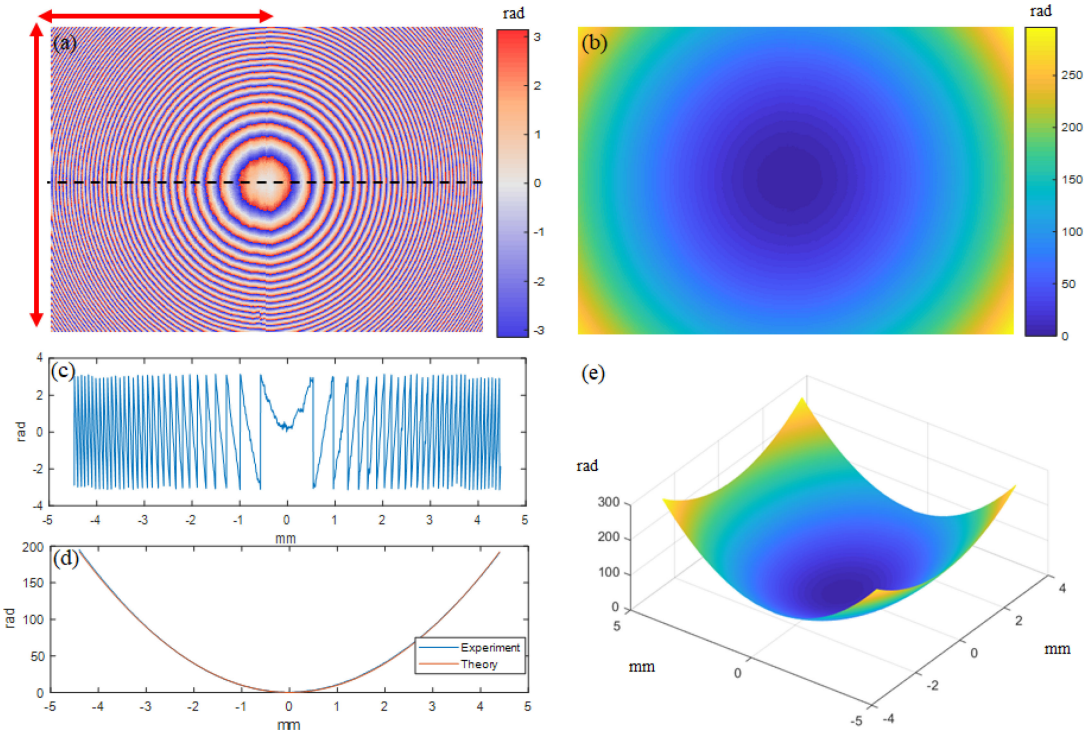

Fig. 6. Quantitative phase imaging using a concave half-mirror. (a) Stitched wrapped phase image. (b) Unwrapped phase profile. (c) Cross section of the wrapped phase along *x*-axis, which corresponds to the black dash line of (a). (d) Unwrapped phase profile of (c) with theoretical value. (e) 3-D distribution of the reconstructed result.

part using wavelength of 650 nm, the resolution limit of our system is 19.94 μm (NA of 0.0326). Therefore, we confirm that SGDH can provide a high-resolution hologram that accords with theoretical diffraction limit.

Next, we carry out another holographic imaging experiment using a latent finger print on slide glass as a specimen to show the potential use of SGDH in the biomedical and forensic fields. The specimen is made by pressing the thumb on the slide glass, mimicking the process of leaving the actual latent fingerprint. Applied to SGDH with multiplexed illumination, the synthesized image is acquired, as shown in Fig. 5(a). Our method reconstructs double FOVs of image without degradation of resolution compared to conventional off-axis DH. Fig. 5(b1) and (c1) are the enlarged images without the numerical propagation of the orange dashed region and yellow dotted region shown in Fig. 5(a). Fig. 5(b2) and (c2) are digitally focused amplitude images that show the core and ridges of fingerprint. Fig. 5(b3) and (c3) are phase images.

Finally, we obtain a phase profile of a concave half-mirror (Thorlabs, CM750-500-G01, focal length is 500 mm) to verify that SGDH provides quantitative phase profile. Fig. 6(a) is the synthesized wrapped phase profile acquired by the proposed method, where the left half is a result for 650 nm and the right half is a result for 670 nm. In order for two phase profiles getting

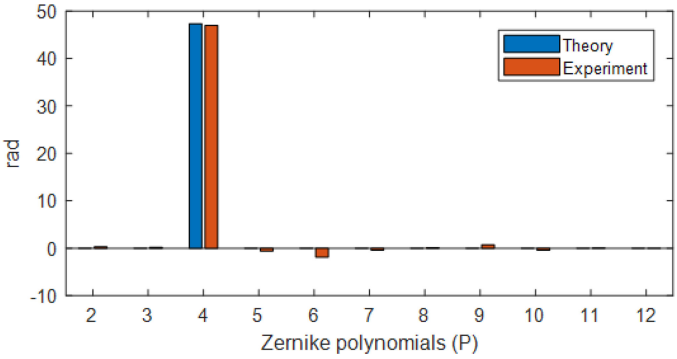

Fig. 7. Zernike polynomials coefficients of the experimental result and theoretical model.

continuous values near the boundary of two images, one of the two phase profiles (e.g., ϕ_{λ_2}) is updated to arg $\{\exp(j\phi_{\lambda_2}) + b\}$, where arg is the phase angle operator, and b is the constant bias. The phase profiles are unwrapped by applying Goldstein algorithm [36] for individual wavelength units. Then, two phase maps of λ_1 and λ_2 are presented with respect to the wavelength of λ_1. The converted phase profiles can be presented by

$$\Phi_{\text{FOV1}} = \Phi_{\lambda_1}$$
$$\Phi_{\text{FOV2}} = \Phi_{\lambda_2} \times \frac{\lambda_1}{\lambda_2} \tag{6}$$

where Φ_λ is an unwrapped phase with wavelength of λ. The unwrapped phase profile that is converted to 650 nm is reconstructed, as shown in Fig. 6(b). Fig. 6(c) plots the cross section of unwrapped phase profile, labeled by black horizontal line shown in Fig. 6(a). In Fig. 6(d), the unwrapped phase profiles of experimental result and theoretical value are shown. It seems that experimental result is in good agreement with the theoretical value. Theoretical phase profile of concave mirror is given by $k\left(x^2 + y^2\right)/2f$, where k is wavenumber and f is focal length of the concave mirror. In addition, we visualize the 3-D distribution of the reconstructed phase profile, which is a quadratic surface, as shown in Fig. 6(e). To quantitatively analyze the phase reconstruction performance, we present the reconstructed result using the Zernike polynomials expansion [37]. The Zernike polynomials correspond to orthogonal optical aberrations such as tilt, astigmatism, defocus, coma, etc. By projecting the reconstructed phase map of the concave mirror to the polynomials, it is possible to confirm how the results are optically accurate. The first 12 orders of the Zernike polynomials coefficients without piston (P = 1) are shown in Fig. 7, using the Fringe indexing scheme [38]. From the bar diagram, the defocus (P = 4) coefficient is the main contribution of the Zernike function for both of theory and experiment. It is a reasonable result because we modeled and measured the spherical mirror. By comparing the relative amplitudes of the coefficients, the optical aberrations of the other terms are negligible and the results are in good agreement with the theory. Fig. 8 shows the phase error between the reconstruction result and the theoretical value on a 2-D image. It seems that the holograms of the two FOVs have continuous phase distributions including the vertical boundary. Most regions show phase errors smaller than 2 rad and the edge

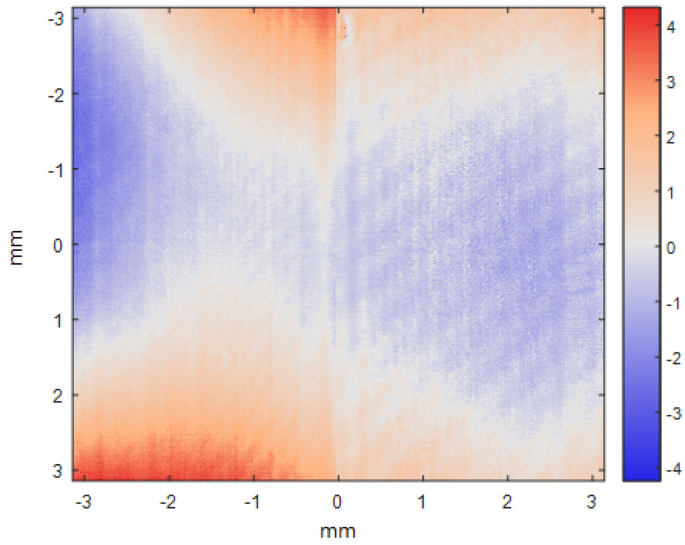

Fig. 8. 2-D phase error between the reconstructed result and the theoretical value.

regions show, where the largest errors appear, about 4 rad. Furthermore, 2-D peak signal to noise ratio of an unwrapped phase image [see Fig. 6(b)] is calculated as 102.64 dB, assuring an accurate reconstruction. From the results, it is confirmed that the proposed method is able to provide quantitative phase profile.

IV. Conclusion

This paper presented a method to implement a simple interferometer for off-axis DH by adopting a diffraction grating. Considering multifunctional application of the grating, the beam splitter and the mirror widely used in conventional off-axis reflective DH were replaced. Furthermore, wavelength dependence of the grating allowed to enhance SBP of the hologram without additional optical components to make multiplexed beams propagate in different directions. The prototype showed a compact design and provided hologram of the diffraction limited resolution and the double FOV. The obtained hologram was digitally propagated to confirm 3-D imaging. Lastly, we demonstrated that SGDH provided quantitative phase profile using a concave half-mirror. We believe SGDH has a potential in various practical use including inspection, identification, cell imaging, and where the compact holographic sensing system with high imaging performance is required.

References

[1] P. Marquet *et al.*, "Digital holographic microscopy: A noninvasive contrast imaging technique allowing quantitative visualization of living cells with subwavelength axial accuracy," *Opt. Lett.*, vol. 30, no. 5, pp. 468–470, 2005.
[2] D. Gabor, "A new microscopic principle," *Nature*, vol. 161, no. 4098, pp. 777–778, 1948.
[3] M. K. Kim, "Principles and techniques of digital holographic microscopy," *J. Photon. Energy*, vol. 1, 2010, Art. no. 018005.
[4] T.-C. Poon, *Digital Holography and Three-Dimensional Display: Principles and Applications*. New York, NY, USA: Springer, 2006.
[5] P. W.-M. Tsang and T.-C. Poon, "Review on the state-of-the-art technologies for acquisition and display of digital holograms," *IEEE Trans. Ind. Inform.*, vol. 12, no. 3, pp. 886–901, Jun. 2016.

[6] E. Cuche, P. Marquet, and C. Depeursinge, "Simultaneous amplitude-contrast and quantitative phase-contrast microscopy by numerical reconstruction of Fresnel off-axis holograms," *Appl. Opt.*, vol. 38, no. 34, pp. 6994–7001, 1999.
[7] J. Min *et al.*, "Dual-wavelength slightly off-axis digital holographic microscopy," *Appl. Opt.*, vol. 51, no. 2, pp. 191–196, 2012.
[8] M. Lee, O. Yaglidere, and A. Ozcan, "Field-portable reflection and transmission microscopy based on lensless holography," *Biomed. Opt. Express*, vol. 2, no. 9, pp. 2721–2730, 2011.
[9] Y. Hu, C. Zuo, J. Sun, Q. Chen, and Y. Zhang, "A compact and lensless digital holographic microscope setup," in *Proc. Int. Conf. Opt. Photon. Eng.*, 2015, vol. 9524, Art. no. 952426.
[10] A. Adinda-Ougba, B. Kabir, N. Koukourakis, F. Mitschker, N. Gerhardt, and M. Hofmann, "Compact low-cost lensless digital holographic microscope for topographic measurements of microstructures in reflection geometry," in *Proc. Opt. Syst. Des. 2015, Opt. Fabr., Testing, Metrology V*, 2015, vol. 9628, Art. no. 962818.
[11] I. Yamaguchi and T. Zhang, "Phase-shifting digital holography," *Opt. Lett.*, vol. 22, pp. 1268–1270, Aug. 1997.
[12] C. Jang, J. Kim, D. C. Clark, S. Lee, B. Lee, and M. K. Kim, "Holographic fluorescence microscopy with incoherent digital holographic adaptive optics," *J. Biomed. Opt.*, vol. 20, no. 11, 2015, Art. no. 111204.
[13] E. Cuche, P. Marquet, and C. Depeursinge, "Spatial filtering for zero-order and twin-image elimination in digital off-axis holography," *Appl. Opt.*, vol. 39, no. 23, pp. 4070–4075, 2000.
[14] J. Hong and M. K. Kim, "Single-shot self-interference incoherent digital holography using off-axis configuration," *Opt. Lett.*, vol. 38, no. 23, pp. 5196–5199, 2013.
[15] B. Lee *et al.*, "Single-shot phase retrieval via Fourier ptychographic microscopy," *Optica*, vol. 5, no. 8, pp. 976–983, 2018.
[16] A. Barty *et al.*, "Ultrafast single-shot diffraction imaging of nanoscale dynamics," *Nature Photon.*, vol. 2, no. 7, pp. 415–419, 2008.
[17] D. Abdelsalam, R. Magnusson, and D. Kim, "Single-shot, dual-wavelength digital holography based on polarizing separation," *Appl. Opt.*, vol. 50, no. 19, pp. 3360–3368, 2011.
[18] J. Kühn *et al.*, "Real-time dual-wavelength digital holographic microscopy with a single hologram acquisition," *Opt. Express*, vol. 15, no. 12, pp. 7231–7242, 2007.
[19] A. Khmaladze, M. Kim, and C.-M. Lo, "Phase imaging of cells by simultaneous dual-wavelength reflection digital holography," *Opt. Express*, vol. 16, no. 15, pp. 10900–10911, 2008.
[20] M. Shan, L. Liu, Z. Zhong, B. Liu, G. Luan, and Y. Zhang, "Single-shot dual-wavelength off-axis quasi-common-path digital holography using polarization-multiplexing," *Opt. Express*, vol. 25, no. 21, pp. 26253–26261, 2017.
[21] M. Paturzo, F. Merola, S. Grilli, S. De Nicola, A. Finizio, and P. Ferraro, "Super-resolution in digital holography by a two-dimensional dynamic phase grating," *Opt. Express*, vol. 16, no. 21, pp. 17107–17118, 2008.
[22] C. Yuan, H. Zhai, and H. Liu, "Angular multiplexing in pulsed digital holography for aperture synthesis," *Opt. Lett.*, vol. 33, no. 20, pp. 2356–2358, 2008.
[23] P. Girshovitz and N. T. Shaked, "Doubling the field of view in off-axis low-coherence interferometric imaging," *Light Sci. Appl.*, vol. 3, no. 3, 2014, Art. no. e151.
[24] B. Tayebi, F. Sharif, M. R. Jafarfard, and D. Y. Kim, "Double-field-of-view, quasi-common-path interferometer using Fourier domain multiplexing," *Opt. Express*, vol. 23, no. 20, pp. 26825–26833, 2015.
[25] I. Frenklach, P. Girshovitz, and N. T. Shaked, "Off-axis interferometric phase microscopy with tripled imaging area," *Opt. Lett.*, vol. 39, no. 6, pp. 1525–1528, 2014.
[26] M. Rubin, G. Dardikman, S. K. Mirsky, N. A. Turko, and N. T. Shaked, "Six-pack off-axis holography," *Opt. Lett.*, vol. 42, no. 22, pp. 4611–4614, 2017.
[27] Y. Lu, Y. Liu, P. Li, Y. Fu, and J. Zhao, "Multiplexed off-axis holography using a transmission diffraction grating," *Opt. Lett.*, vol. 41, no. 3, pp. 512–515, 2016.
[28] W. Zhang, L. Cao, G. Jin, and D. Brady, "Full field-of-view digital lensfree holography for weak-scattering objects based on grating modulation," *Appl. Opt.*, vol. 57, no. 1, pp. A164–A171, 2018.
[29] W.-C. Hsu, J.-W. Su, T.-Y. Tseng, and K.-B. Sung, "Tomographic diffractive microscopy of living cells based on a common-path configuration," *Opt. Lett.*, vol. 39, no. 7, pp. 2210–2213, 2014.
[30] V. Mico, C. Ferreira, Z. Zalevsky, and J. García, "Spatially-multiplexed interferometric microscopy (SMIM): Converting a standard microscope into a holographic one," *Opt. Express*, vol. 22, no. 12, pp. 14929–14943, 2014.
[31] G. Popescu, T. Ikeda, R. R. Dasari, and M. S. Feld, "Diffraction phase microscopy for quantifying cell structure and dynamics," *Opt. Lett.*, vol. 31, no. 6, pp. 775–777, 2006.
[32] B. Bhaduri *et al.*, "Diffraction phase microscopy: Principles and applications in materials and life sciences," *Adv. Opt. Photon.*, vol. 6, no. 1, pp. 57–119, 2014.
[33] W. Bishara, T.-W. Su, A. F. Coskun, and A. Ozcan, "Lensfree on-chip microscopy over a wide field-of-view using pixel super-resolution," *Opt. Express*, vol. 18, no. 11, pp. 11181–11191, 2010.
[34] A. Greenbaum *et al.*, "Wide-field computational imaging of pathology slides using lens-free on-chip microscopy," *Sci. Transl. Med.*, vol. 6, no. 267, 2014, Art. no. 267ra175.
[35] V. Bianco *et al.*, "Endowing a plain fluidic chip with micro-optics: A holographic microscope slide," *Light Sci. Appl.*, vol. 6, no. 9, 2017, Art. no. e17055.
[36] R. M. Goldstein, H. A. Zebker, and C. L. Werner, "Satellite radar interferometry: Two-dimensional phase unwrapping," *Radio Sci.*, vol. 23, no. 4, pp. 713–720, 1988.
[37] Z. von F, "Beugungstheorie des schneidenver-fahrens und seiner verbesserten form, der phasenkontrastmethode," *Physica*, vol. 1, no. 7–12, pp. 689–704, 1934.
[38] V. L. Genberg, G. J. Michels, and K. B. Doyle, "Orthogonality of Zernike polynomials," in *Proc. Optomechanical Des. Eng.*, 2002, vol. 4771, pp. 276–287.

Byounghyo Lee received the B.S. degree in electrical engineering in 2015 from Seoul National University, Seoul, South Korea, where he is currently working toward the Ph.D. degree in holographic imaging.

His research interests include digital holography, 3-D microscopy, phase retrieval, 3-D display, augmented reality, and near-eye displays.

Changwon Jang received the Ph.D. degree in electrical engineering from Seoul National University, Seoul, South Korea, in 2018.

His primary research interests include 3-D display and digital holography.

Dongyeon Kim received the B.S. degree in electrical engineering in 2017 from Seoul National University, Seoul, South Korea, where he is currently working toward the M.S. degree in three-dimensional display.

His research interests include 3-D displays, digital holography, augmented reality, and near-eye displays.

Byoungho Lee (M'94–SM'00–F'14) received the Ph.D. degree from the Department of Electrical Engineering and Computer Science, University of California, Berkeley, CA, USA, in 1993. He is currently a Professor and the Head with the School of Electrical and Computer Engineering, Seoul National University, Seoul, South Korea.

Dr. Lee was the recipient of many awards, including the Jin-Bo-Jang Medal from the President of South Korea in 2016. He was on the Board of Directors of OSA, and a Senior Member of the National Academy of Engineering of Korea. He was the Vice-President of the Korean Information Display Society. He is currently a member of the Korean Academy of Science and Technology, and also the President of the Optical Society of Korea. He is a Fellow of SPIE and the Optical Society of America.